International Journal of Pharmaceutics 678 (2025) 125710

Contents lists available at ScienceDirect

International Journal of Pharmaceutics

journal homepage: www.elsevier.com/locate/ijpharm

Cannabidiol-loaded-injectable depot formulation for the treatment of triple-negative breast cancer: design, development, in-vitro and in-ovo evaluation of its anticancer activity☆

Irene Lozza [a], Cristina Martín-Sabroso [a,b], Carolina Hurtado-Marcos [c], Consuelo Montejo-Rubio [c], Ana Isabel Fraguas-Sánchez [a,b,*], Ana Isabel Torres-Suárez [a,b,*]

[a] Department of Pharmaceutics and Food Technology, Faculty of Pharmacy, Complutense University of Madrid, Spain
[b] Institute of Industrial Pharmacy. Faculty of Pharmacy, Complutense University of Madrid, Spain
[c] Department of Health and Pharmaceutical Sciences, School of Pharmacy, Universidad San Pablo-CEU, CEU Universities, Spain

ARTICLE INFO

Keywords:
Breast cancer
Cannabinoids
Drug delivery
Injectable formulations
In situ forming implants

ABSTRACT

Triple-negative breast cancer (TNBC) is an invasive and difficult-to-treat carcinoma that represents 15–20 % of breast malignancies and is frequently diagnosed in younger women. Chemotherapy is the mainstay treatment approach. Cannabidiol (CBD), the main non-psychoactive cannabinoid, has shown a potential anticancer activity in TNBC, enhancing the effect of conventional antineoplastics. This research aims to develop in situ forming implants (ISFIs) as a long-acting depot formulation of CBD with potential application in TNBC. This formulation is intended to be administered in the tumor site during neoadjuvant chemotherapeutic regimens, allowing a controlled CBD release. ISFIs were elaborated with 100 mg of polycaprolactone (PCL) and 2.5 mg (2.5-CB-ISFI), 5 mg (5-CB-ISFI) or 10 mg (10-CB-ISFI) of CBD dissolved in 400 µL of NMP. All the formulations exhibited a controlled drug release for around two months. 10-CB-ISFI formulation with the highest CBD content and the most suitable CBD release profile was selected for biological studies. This formulation inhibited the proliferation and migration of MDA-MB-231 and 4T1 cells and exerted an antiangiogenic effect in ovo. Interestingly, the antiangiogenic activity of 10-CB-ISFI was higher compared with CBD in solution administered at the same concentration, showing vascular inhibition percentages of around 80 % and 60 %, respectively. Finally, this formulation reduced the growth of MDA-MB-231-derived tumors developed in the chorioallantoic membrane (CAM) model. The single administration of 10-CB-ISFI exhibited a similar antitumor efficacy to the daily administration of CBD in solution (≈60 % tumor growth inhibition). Therefore, the injectable depot formulation of CBD developed in this work showed a promising utility in TNBC treatment.

1. Introduction

Breast cancer (BC) is the most common cancer in women worldwide, accounting for approximately 11.6 % of new cancer diagnoses in this population, and represents a leading cause of cancer-related deaths (Barzaman et al., 2020; Bray et al., 2024). It can be categorized into three groups based on their molecular patterns: i) Hormone-Receptor-expressing BC that express estrogen receptors and/or progesterone receptors, ii) Human Epidermal Receptor type 2 (HER-2) expressing BC, and iii) Triple-negative breast Cancer (TNBC) that lacks estrogen, progesterone, and HER-2 receptors (Clusan et al., 2021).

TNBC represents approximately 15–20 % of all breast malignancies, being frequently diagnosed in younger women, especially those under 50 years old. While breast tumors expressing progesterone or estrogen receptors, in general, respond well to hormone therapy and those overexpressing HER-2 are effectively treated with HER-2 targeted therapies, TNBC does not respond to these treatments, so fewer treatment options are available (Obidiro et al., 2023; Yin et al., 2020). Nowadays, chemotherapy remains the mainstay pharmacotherapy for TNBC. It is often administered before surgery (neoadjuvant chemotherapy) to reduce the tumor size and/or after surgery (adjuvant chemotherapy) to kill any remaining tumor cells and reduce the chance

☆ This article is part of a special issue entitled: 'Parenteral Time-Controlled Drug Delivery' published in International Journal of Pharmaceutics.

* Corresponding authors at: Department of Pharmaceutics and Food Technology, Complutense University of Madrid, Spain.
E-mail addresses: aifraguas@ucm.es (A.I. Fraguas-Sánchez), galaaaa@ucm.es (A.I. Torres-Suárez).

https://doi.org/10.1016/j.ijpharm.2025.125710
Received 13 January 2025; Received in revised form 29 April 2025; Accepted 9 May 2025
Available online 9 May 2025

of recurrence (Ulhaka et al., 2021; Xiong et al., 2024). Moreover, TNBC often grows and spreads more rapidly than other types of BC, leading to a poorer prognosis and a higher likelihood of recurrence (Sukumar et al., 2021). All this makes TNBC a significant health problem.

In recent decades, cannabinoids have garnered a great deal of attention as potential therapeutic agents in cancer disease (Coelho et al., 2023; Fraguas Sánchez and Torres-Suarez, 2023). Several Cannabis sativa-based preparations (such as Tilray®, Bediol®, Bedrocan® and Bedica®) are currently available in Australia, Canada and some countries of Europe as palliative agents to treat nausea and vomiting related to chemotherapy. Moreover, the Food and Drug Administration (FDA) has approved three medications containing dronabinol, synthetic Δ^9-THC (Marinol® and Syndros®) or nabilone, Δ^9-THC analog (Cesamet®), as active for this purpose (Bimonte et al., 2024; Skórzewska and Gęca, 2024). Cannabinoids have also demonstrated anticancer activity per se by inhibiting tumor growth and metastases and exerting an anti-angiogenic effect (Bathula and Maciver, 2024).

Cannabidiol (CBD) is the most abundant non-psychoactive cannabinoid and has shown promising antitumor activity in breast cancer, including TNBC (Heider et al., 2022; Yan et al., 2023). Numerous research works have demonstrated that CBD inhibits the proliferation of TNBC cells by inducing apoptosis and generating Reactive Oxygen Species (ROS). Moreover, it reduces the invasiveness of tumor cells, down-regulating the activity of Inhibitor Differentiation Protein 1 (ID-1) (Bimonte et al., 2023), which is overexpressed in TNBC and associated with larger tumor sizes, higher invasiveness, and poorer prognosis (García-Escolano et al., 2021). Furthermore, it has been reported that CBD enhances the efficacy of conventional antineoplastic drugs such as paclitaxel and doxorubicin (Fraguas-Sánchez et al., 2023; Surapaneni et al., 2022). For example, Patel and collaborators demonstrated in a xenograft tumor model of TNBC (developed by injecting MDA-MB-231 cells) that CBD encapsulated in extracellular vesicles at doses of 5 mg/Kg significantly improved the antitumor efficacy of doxorubicin administered at doses of 2 mg/Kg (Patel et al., 2021). Moreover, CBD alleviates some of the major side effects associated with these antineoplastics, like the peripheral neuropathy of paclitaxel and cardiotoxicity of doxorubicin (Buchtova et al., 2023; Hao et al., 2015; Kumar Kalvala et al., 2022), reinforcing the utility of combining CBD and conventional antineoplastics.

Nevertheless, CBD exhibits high lipophilicity (Log P 6.3), high instability and low and erratic oral bioavailability. All this complicates its handling and administration, making drug delivery systems an interesting strategy to administer this drug (Fraguas-Sánchez et al., 2024).

In-situ forming implants (ISFIs), defined as liquid formulations that form solid or semi-solid depots upon the administration site, have garnered significant interest as long-acting formulations becoming an alternative to traditional surgical implants (Wang and Burgess, 2021) due to, among other advantages, their simple manufacturing process, their easy and simple administration way to patients and their ability to control drug release over extended periods (from days to months depending on the formulation) (Suh et al., 2021) which allows a long-lasting effect with a single administration. This prolonged activity is worth considering in the treatment of cancer, where there is a need for prolonged therapies (Ibrahim et al., 2021; Pandya et al., 2023).

ISFIs can be classified according to their formation mechanism at the injection site into thermally induced systems, pH-responsive formulations, cross-linked implants and systems based on phase separation due to solvent exchange (Dubar et al., 2021). The solvent exchange process is one of the most used mechanisms of formation, consisting of the precipitation of the polymer in solution and the formation of a deposit at the injection site because of the diffusion of the solvent into the surrounding tissues and the penetration of water into the formulation. The drug is entrapped into this deposit (Gomaa et al., 2023). The FDA and/or the European Medicines Agency (EMA) have approved several ISFI formulations based on this mechanism: i) Eligard® a formulation of leuprorelin approved for the treatment of prostate cancer, ii) Sublocade® and Brixadi® (approved by EMA as Buvidal®), ISFIs that contain buprenorphine used for opioid dependence, iii) Perseris®, Uzedy® and Risvan® (EMA approved this latter as Okedi®) that consist of formulations of risperidone approved for schizophrenia and iv) Atridox® that contains doxycycline hyclate and is used for the treatment of periodontitis. Except for Brixadi®, prepared with soybean phosphatidylcholine/glycerol dioleate, all these formulations contain polylactide (PLA) or poly-lactic-co-glycolic acid (PLGA) as polymeric matrix dissolved in N-methyl-2-pyrrolidone (NMP) or dimethyl sulfoxide (Kanwar and Sinha, 2019; Lim et al., 2022; Markowicz-Piasecka et al., 2024).

This research aims to design, develop, and characterize CBD-loaded ISFIs as a long-acting injectable formulation with potential application in treating TNBC. This formulation is intended to be administered in the tumor area during neoadjuvant chemotherapy before the surgical removal of the tumor This formulation is composed of polycaprolactone (PCL), an aliphatic polyester polymer widely used in the development of drug delivery systems, as it is a biodegradable and highly biocompatible polymer (Pawar et al., 2023), and NMP as a water-soluble solvent. To the best of our knowledge, this is the first work to develop a PCL-based injectable depot implant to administer cannabinoids and to evaluate their utility in inhibiting the proliferation and migration of breast tumors.

2. Materials and methods

2.1. Materials

Polycaprolactone (PCL) (Resomer® C202, average MW: ≈12000, Inherent Viscosity 0–2–0.26 dL/g) was obtained from Evonik® Industries (Essen, Germany). Cannabidiol was supplied by THC Pharm (Frankfurt, Germany). Sodium phosphate dibasic dihydrate ($Na_2HPO_4{\cdot}2H_2O$), Potassium dihydrogen phosphate (KH_2PO_4), and Polyethylene glycol sorbitan monooleate (Tween 80) were purchased from Panreac (Barcelona, Spain). Carboxymethylcellulose sodium salt (high viscosity) and glycerol were obtained from Sigma Aldrich (Missouri, USA) NMP, Gibco™ RPMI 1640 medium, Gibco™ Trypsin-EDTA (0.25 %), Mitomycin C, Gibco™ PBS pH 7.4, Gibco™ Fetal Bovine Serum (FBS), Gibco™ Geltrex Matrix and Molecular Probes™ MTT (3-(4,5-dimethylthiazole-2-yl)-2,5-diphenyltetrazolium bromide) were obtained from Fisher Scientific (Madrid, Spain). Methanol and acetonitrile were purchased from Scharlab S.L. (Barcelona, Spain). Milli-Q® water was obtained using a Millipore system (Massachusetts, USA).

2.2. Injectability and viscosity studies

ISFIs were prepared using PCL as polymer and NMP as solvent. Firstly, the injectability and viscosity of the polymeric solutions at different polymer: solvent ratios (w/v) (100 mg:150 μL, 100 mg:300 μL, or 100 mg:400 μL) were analyzed.

The injectability was tested in a double-blinded study. Briefly, seven volunteers were asked to evaluate the injectability of 1 ml of each solution in 1 mL syringes (Injekt-F, B-Braun, Germany) coupled with 23G and 25G needles and assign a score (ranging from 1 to 4) to each sample based on the ease of injectability and the flow through the needle: score 1: injectability extremely hard and no-flow; score 2: injectability hard and flow starts with droplets, then steady; score 3: injectability relatively easy and flow steady and score 4: injectability very easy and flow steady. Prior to this experiment, the volunteers were trained with standard solutions: i) solution of carboxymethylcellulose sodium salt in water (viscosity range at 25 °C of 400–800 cps) as difficult to inject reference, ii) solution of glycerol in water at 85 % (viscosity at 25 °C of ≈100Cp), as moderate to inject reference and iii) MiliQ water as easy to inject reference.

A DVNext Brookfield Ametek (Massachusetts, USA) viscosimeter

equipped with a CP42 cone spindle was used to evaluate the apparent viscosity of 1 mL of each polymeric solution as the shear rate increased and decreased sequentially (0–26.88–0 s^{-1}). Viscosity data were collected using Rheocalc DVNXRVCJG 2.1.8.3–9 software.

2.3. Elaboration of ISFIs

CBD-loaded ISFIs (CB-ISFI) were elaborated by the direct medium injection technique. PCL (100 mg) and CBD (2.5, 5, or 10 mg) were dissolved in 400 μL of NMP. Then, 200 μL of each solution was injected into a vial containing 5 ml of phosphate buffer (PBS) pH 7.4 using a standard 25G needle gauge syringe. Formulations without CBD (PCL-ISFI) were also prepared.

2.4. Characterization of ISFIs

2.4.1. Morphology

Implant morphology was examined by both optical microscopy (Ninyoon 4K microscope, Evatost, Ireland) and scanning electron microscopy (SEM) (JEOL 6400 JSM, Tokyo, Japan) 15 min after ISFIs preparation as described above (section 2.3). The excess water was removed before examination. For optical microscopy, implants were directly examined (Ninyoon 4K microscope, Evatost, Ireland). However, for SEM analyses, the implants were placed onto aluminum stubs, dried for 48 h in a desiccator, and coated with gold for 180 s.

2.4.2. Drug release

The release from ISFIs prepared with 2.5 mg (2.5-CB-ISFI), 5 mg (5-CB-ISFI), and 10 mg (10-CB-ISFI) of CBD was evaluated in PBS pH 7.4 containing Tween 80 at 1 % to maintain sink conditions. Implants were prepared by injecting 200 μL of each CBD-PCL solution in NMP into glass-closed tubes containing 5 mL of release medium. Then, they were placed in a thermostatic water shaking bath (ST 30 Nuve Sanayi, Turkey) maintained at 37 ± 0.5 °C and 100 rpm. At specific times (15 min, 1 h, 2 h, 6 h, 1, 2, 4, 7, 14, 21, 28, 35, 49, and 60 days), the supernatant was gently removed and filtered with 0.45 μm cellulose syringe filters. Fresh-release medium was added at each time (Lozza et al., 2024). The samples were then analyzed by HPLC (Fraguas-Sánchez et al., 2020b).

2.5. Cell culture studies

2.5.1. Cell lines

MDA-MB-231 (ATCC HTB-26, human origin) and 4T1 (CRL-2539, mouse origin) cell lines were selected as models of TNBC. Both cells were cultured in RPMI-1640 medium supplemented with 10 % (v/v) FBS and 1 % (v/v) penicillin–streptomycin and incubated at 37 °C and 5 % CO_2.

2.5.2. Antiproliferative activity

MDA-MB-231 cells were seeded in 6-well plates at a density of 350,000 cells per well. 24 h after seeding, the medium was removed, and cells were treated with complete cell culture medium (RPMI-1640) and CBD treatments (CBD in solution and 10-CB-ISFIs) at a CBD concentration of 15 μM for 48 h. Similarly, 4T1 cells were seeded at a density of 150,000 cells per well and treated 24 h post-seeding with either complete cell culture medium (RPMI-1640) and CBD treatments (CBD in solution and 10-CB-ISFIs) at a CBD concentration of 7.5 μM for 48 h. These concentrations were selected based on the IC_{50} values of CBD in solution determined for each cell line (see Supplementary material, Figs. S1 and S2). Cells treated only with cell culture medium served as control.

For this study, 10-CB-ISFIs were formed in parallel in separate plates and maintained in complete cell culture medium at 37 °C. At predetermined time points after their formation, 0 days (recently prepared implants, T0-2), 2 days (T2–4), 4 days (T4–6), and 6 days (T6–8) implants were collected. Then, the cells were treated with these collected implants for 48 h. The effect of freshly prepared (T0-2) unloaded PCL-ISFIs was also evaluated to verify the toxicity attributed to the formulation.

48 hours after treatment, the implants were gently removed, and cells were washed with PBS. Cell viability was then assessed using the MTT assay. Briefly, 600 μL of MTT solution in complete RPMI-1640 medium (1.0 mg/mL) were added to each well. After 3 h of incubation, the medium was carefully removed, and 600 μL of DMSO were added to each well to solubilize the formazan crystals. The plates were gently agitated for 10 min at 100 rpm, and absorbance was measured at 570 nm using a plate reader spectrophotometer (Varioskan LUX, Thermo Fisher Scientific, Madrid, model 3020-2023).

2.5.3. Migration study: scratch assay

The effect of CBD and 10-CB-ISFIs on cell migration was assessed using the scratch assay (Duchesne et al., 2018). Briefly, MDA-MB-231 and 4T1 cells were seeded in 24-well plates at a cell density of 50,000 cells/well and 30,000 cells/well, respectively. When 90–100 % of confluence was reached, the cells were treated with mitomycin (10 μg/mL) for 40 min to stop cell proliferation. Then, each well was scraped with a sterile 10 μL pipette tip, and the cells were washed with PBS to remove cellular debris. Then, CBD in solution and 10-CB-ISFI (recently prepared in complete cell culture medium) were administered at a CBD concentration of 5 and 7.5 μM in 4T1 cells and 10 μM and 20 μM in MDA-MB-231 cells. These CBD concentrations showed a cell death lower than 30 % after 24 h of treatment (Supplementary material Figs. S1 and S2). Cells treated with a complete RPMI medium were used as controls. Cells were photographed before (T0) and 24 h after the administration of each treatment (T24) using a microscope Eclipse TE300 Nikon microscope (Melville, USA). The percentage of wound closure was calculated using ImageJ-Fiji software using the following equation:

$$Wound\ closure(\%) = \frac{\text{Area T0} - \text{Area T24}}{AreaT0} \times 100 \quad (1)$$

The migration ratio of each treatment was also calculated as follows:

$$Migration\ ratio = \frac{\text{Wound closure treatment}}{Wound\ closure\ control} \quad (2)$$

2.6. In ovo studies

2.6.1. Angiogenesis study

The antiangiogenic effect of 10-CB-ISFIs was studied in the chorioallantoic membrane (CAM) model (Alonso-González et al., 2022). Briefly, fertilized leghorn chicken eggs (Granja Santa Isabel, Cordoba, Spain) were incubated at 37 °C and 47 % humidity. On embryo development day 4 (EDD4), the eggshell was gently drilled, and the hole was sealed with tape. On EDD 10, the CAM was exposed, and a silicone O-ring with a diameter of 1 cm was positioned on this membrane to define the treatment area. The eggs were then treated for 48 h with CBD in solution at 100 μM (daily administration of 7.78 μg of CBD dissolved in RMPI-medium) or the equivalent amount of 10-CB-ISFIs (single administration of 4.5 μL of CBD-ISFI polymeric solution to get a CBD release of around 16 μg in 48 h). Eggs treated with PCL-ISFIs and PBS pH 7.4 (negative control for angiogenesis) were also evaluated. The treated area of each egg was photographed 48 h after the treatments and analyzed by calculating the total number of blood vessels and the vascular density (Sabaner et al., 2021).

Vascular density was calculated using ImageJ-Fiji software. Firstly, images were converted to an 8-bit image type, and the threshold was adjusted. Then, vascular density was automatically calculated according to the black-and-white color differences ratio.

2.6.2. Antitumor efficacy

The antitumor efficacy of CBD-ISFIs was also tested in ovo in MDA-MB-231-derived tumors formed onto the CAM. Fertilized leghorn

chicken eggs were incubated as described in section 2.6.1. On EDD 4, the eggshell of each egg was carefully drilled and closed with tape [33]. On EDD 7, the hole was opened, and CAM was exposed. Then, it was gently scratched, and MDA-MB-231 cells (2 x 10^6 cells suspended in Geltrex® matrix, 30 μL per egg) were inoculated. On EDD 9, MDA-MB-231-derived tumors were already formed. They were surrounded with a silicone o-ring (1 cm in diameter), photographed (Ninyoon 4K microscope, Evatost, Ireland) and topically treated with PBS pH 7.4 (used as negative control), CBD in solution (daily administration of 7.78 μg of CBD dissolved in RMPI-medium), 10-CB-ISFI (single administration of 4.5 μL of CBD-ISFI polymeric solution to get a CBD release of around 16 μg in 48 h) or PCL-ISFI (single administration of 4.5 μL of PCL solution without CBD). On EDD 11, the tumors were photographed again.

The tumor growth (%) was obtained by calculating the tumor area before (Tumor area initial) and after (Tumor area final) the treatments using ImageJ-Fiji software as follows (Fraguas-Sánchez et al., 2020c):

$$Tumour\ growth(\%) = \frac{\text{Tumor area final}}{Tumor\ area\ initial} \times 100 \quad (3)$$

2.7. Statistical analysis

Data are displayed as mean ± standard deviation (SD) of at least three independent experiments. Cell culture studies were performed in quadruplicate, and in the studies in ovo, at least 5 eggs per treatment were analyzed. The injectability study scores were statistically compared using the Mann-Whitney *U* test using IBM SPSS Statistics 28 software (IBM, Chicago, Illinois). In the rest of the experiments, the significance of the differences detected between the two groups was evaluated using a student's *t*-test. ANOVA test was used to compare the differences detected between multiple groups. Both tests were performed using Statgraphics 19 Centurion (Statgraphics Technologies, Inc., The Plains, Virginia). Finally, the graphs were elaborated using Origin 2019 software (OriginLab, Massachusetts, USA).

3. Results and discussion

3.1. Injectability and viscosity studies

The injectability and viscosity of the polymeric solutions were first examined to determine the most suitable polymer:solvent ratio for preparing CB-ISFIs. Table 1 displays the scores obtained from the injectability study in which volunteers scored the ease of injectability and the flow of the different polymeric solutions (100 mg of PCL dissolved in 150, 300 or 400 μL of NMP) through 23G and 25G needles and the results of viscosity measurements. Only in the solutions prepared with 100 mg of PCL and 400 μL of NMP, all participants indicated good injectability properties (score 3 or 4) through 23G and 25G needle gauges without detecting statistically significant differences between both needles (p-value > 0.05). The better injectability properties of this solution can be attributed to its lower viscosity. While the PCL solution prepared with a PCL: NMP ratio of 100 mg:400 μL showed a mean viscosity value of around 65 cP, the solutions elaborated with a lower volume of NMP showed a significantly higher viscosity above 100 cP. Therefore, a PCL:NMP ratio of 100 mg:400 μL was selected to prepare CB-ISFIs.

Table 1
Results of injectability and viscosity studies.

Polymer: solvent ratio	Injectability study			Viscosity (cP) Mean ± SD (n = 3)
	Score range (median) 23G needle (n = 7)	Score range (median) 25G needle (n = 7)	Suitable Injectability	
100 mg:150 μL	1–2 (1)	1–2 (1)	No	582.23 ± 2.54
100 mg:300 μL	2–3 (3)	2–3 (3)	No	134.05 ± 3.85
100 mg:400 μL	3–4 (4)	3–4 (4)	Yes	65.6 ± 1.10

3.2. Elaboration and characterization of ISFIs

CB-ISFIs were elaborated with 100 mg of PCL and 2.5 mg (2.5-CB-ISFI), 5 mg (5-CB-ISFI) or 10 mg (10-CB-ISFI) of CBD dissolved in 400 μL of NMP. All these solutions were clear and transparent to yellowish. When these solutions were injected into the simulated physiological medium (PBS, pH 7.4) all the implants were rapidly formed.

3.2.1. Optical and SEM microscopy

Fig. 1 displays the appearance of recently prepared ISFIs. All the formulations exhibited an irregular shape, typical of the implants elaborated by the direct injection technique (Zhang et al., 2019). No differences were observed in the aspect of PCL-ISFIs and CB-ISFIs, nor in the appearance of the implants prepared with varying amounts of CBD.

When the surface of the implants was examined by SEM (Fig. 2), a smooth surface was observed in both unloaded and CBD-loaded ISFIs. It should be noted that some pores can be appreciated on the surface of all the formulations, which are attributed to the removal of the solvent during the solidification process. NMP is a hydrophilic solvent that rapidly diffuses into the aqueous medium when the polymeric solution is injected into an aqueous environment, triggering the formation of porous implants (Thakur et al., 2014). It has been demonstrated that the faster solvent removal, the higher porosity of the polymeric matrix. Unloaded PCL-ISFIs showed a more porous surface than CBD-loaded formulations, probably due to the plasticizer effect of CBD on PCL [45].

3.2.2. In vitro drug release study

As depicted in Fig. 3, CBD-loaded ISFIs exhibited a controlled drug release over approximately 60 days, with more than 80 % of CBD being released by this time. Typically, the higher the drug content, the higher the release rate. For instance, in PLGA-ISFIs loaded with cabotegravir, the release rate of this drug increased from 3.35 to 11.20 μg/day in implants prepared with drug concentrations of 112 and 290 mg/ml, respectively (Young et al., 2023). Similar results were found in PLGA implants prepared with 10 % and 20 % of insulin (w/w) (Jensen et al., 2016). However, CB-ISFIs showed an inverse relationship: the higher the CBD content, the slower the drug release. This aspect could be related to the plasticizer effect of this cannabinoid on PCL [45]. It should be noted that this phenomenon has also been appreciated in other CBD-loaded polymeric formulations. For example, in microparticles containing 10 % (w/w) of CBD, around 60 % of this cannabinoid was released within 21 days, whereas in formulations with 20 % (w/w) of CBD, this release percentage was achieved in 31 days (Fraguas-Sánchez et al., 2020a).

2.5-CB-ISFIs exhibited the fastest drug release with a relatively high burst effect; approximately 40 % of the CBD was released within the first 48 h. The burst effect in 5-CB-ISFIs and 10-CB-ISFIs was significantly lower, with around 28 % and 18 % of the CBD released by this time. Both 2.5-CB-ISFIs and 5-CB-ISFIs showed a biphasic release profile with an initial first faster release phase from day 2 to day 7 (around 57 % and 47 % of the CBD was released after 7 days from 2.5-CB-ISFIs and 5-CB-ISFIs respectively), followed by a second phase up to day 60 in which CBD is released slowly. This second phase can be fitted to a zero-order release kinetics (2.5-CB-ISFIs: $K_0 = 7.325$ μg/day, $R^2 = 0.9857$; 5-CB-ISFIs $K_0 = 18.62$ μg/day, $R^2 = 0.9806$). Nevertheless, the CBD release from 10-CB-ISFIs was more controlled, detecting a constant release phase from day 2 to day 60 fitted to zero-order release kinetics ($K_0 = 53$ μg/day, $R^2 = 0.967$).

A previous study showed that CBD-loaded ISFIs prepared with other polymers (PLGA-502, PLGA-502H or PLA-202) exhibited a notably faster CBD release than the PCL formulations developed in this work.

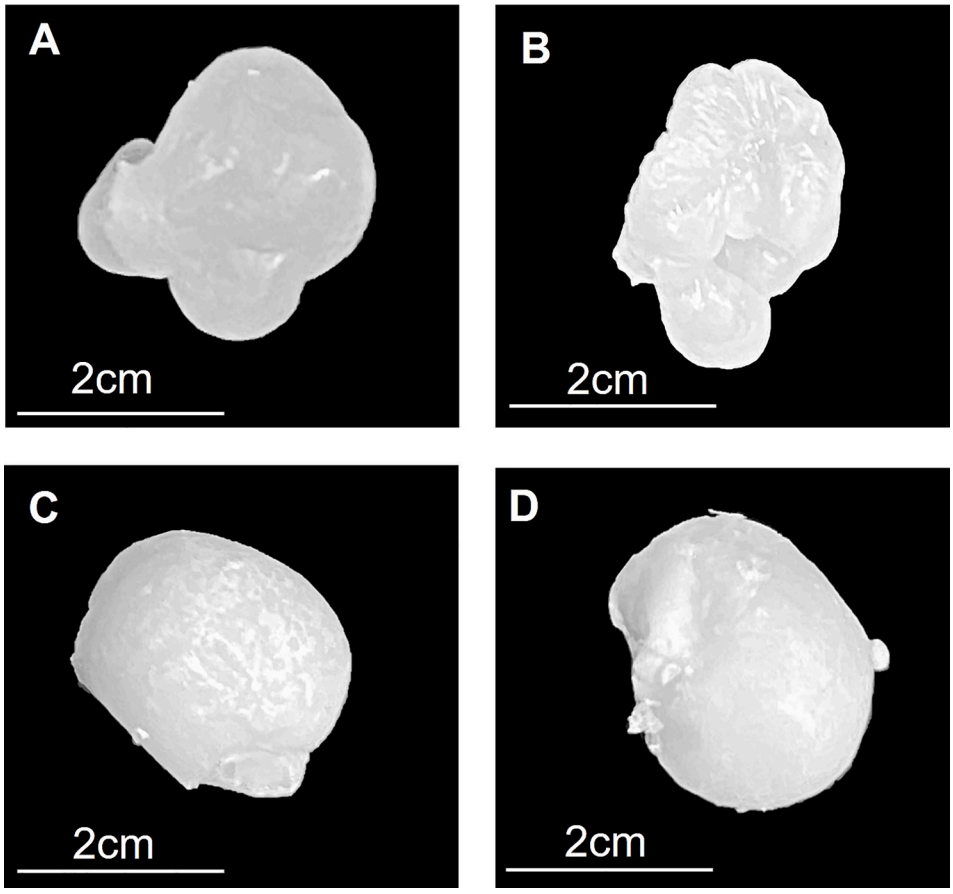

Fig. 1. Optical images of recently prepared PCL-ISFI (A), 2.5-CB-ISFI (B), 5-CB-ISFI (C) and 10-CB-ISFI (D) formulations.

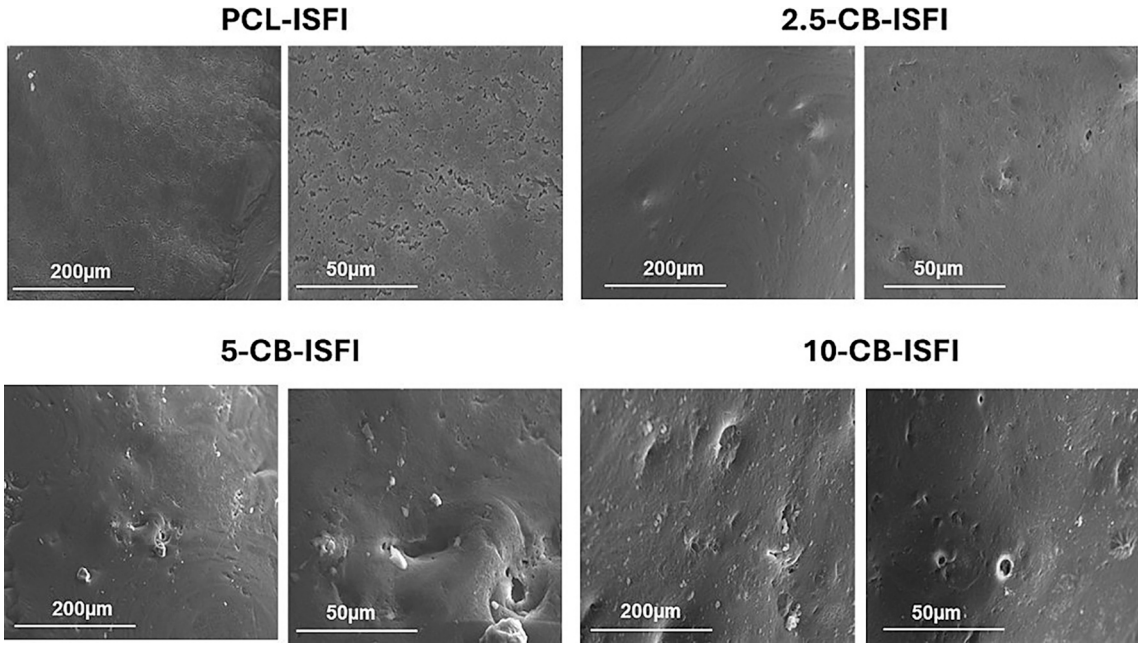

Fig. 2. Surface morphology of PCL-ISFIs and CB-ISFI implants examined by SEM.

PLGA and PLA ISFIs were prepared at two different CBD-polymer ratios: 2.5:100 and 5:100. While PCL-ISFIs exhibited less than 30 % of CBD released within the first day, PLGA and PLA formulations released more than 45 % of this cannabinoid by this time (Lozza et al., 2024). This difference could be attributed to the crystallinity of the polymers. While PLGA and PLA are amorphous, PCL is semicrystalline (Bhadran et al., 2023; Gentile et al., 2014), and drug release is usually faster in polymers with higher amorphous content due to the difficulty of water

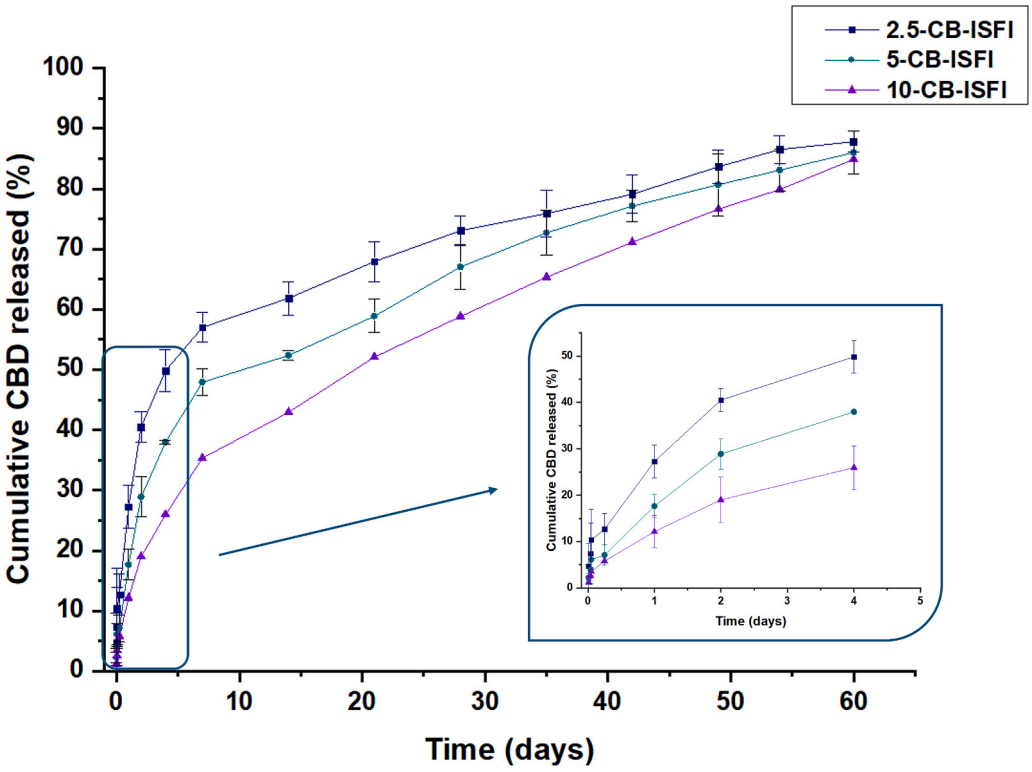

Fig. 3. Drug release profile of CBD-loaded-ISFIs.

penetration, which is responsible for the bulk erosion of the polymer (Miles et al., 2021).

3.3. Cell culture experiments

CBD has attracted considerable interest because of its potential anticancer properties, as it inhibits the proliferation, migration, and invasion of cancer cells and reduces tumor growth and metastases (Nahler, 2022). One tumor where it has excellent potential is breast cancer, including TNBC. This study evaluated the antiproliferative and antimigration activity of 10-CB-ISFIs in MDA-MB-231 and 4T1 cells. This formulation was selected as it showed the highest CBD content (10 mg per 100 mg of polymer) and exhibited the most suitable CBD release profile (lowest burst effect and more controlled CBD release for around 60 days). This controlled drug release would provide a long-acting effect with a single administration.

3.3.1. Antiproliferative activity

The antiproliferative activity of 10-CB-ISFIs was evaluated for 8 days. For this study, MDA-MB-231 and 4T1 cells were treated with CBD in solution and with 10-CB-ISFI at a drug concentration of 15 μM and 7.5 μM, respectively. These concentrations correspond approximately to the IC_{50} values (16.5 μM ± 5.2 in MDA-MB-231 cells and 7.4 μM ± 3.4 in 4T1 cells) of CBD in solution after 48 h of incubation in both cell lines (Fig. S1 and S2). The cytotoxicity of PCL-ISFIs was also tested.

While PCL-ISFIs did not exhibit cytotoxic effects in MDA-MB-231 and 4T1 cells, 10-CB-ISFIs demonstrated a prolonged and constant antiproliferative activity for at least 8 days (Fig. 4). 10-CB-ISFIs showed a lower antiproliferative activity (cell death percentage of around 25 % and 30 % in MDA-MB-231 and 4T1 cells, respectively) than CBD in

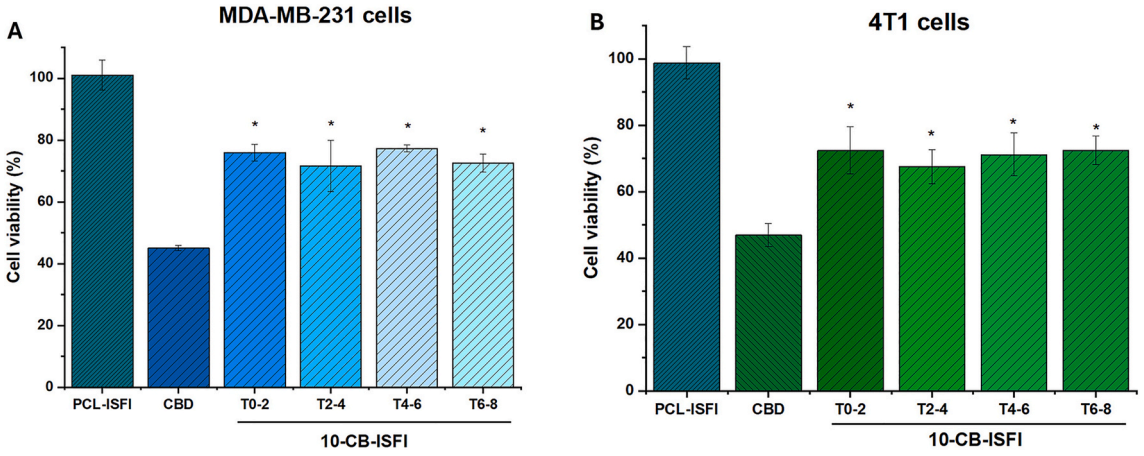

Fig. 4. Cell viability studies of 10-CB-ISFIs in MDA-MB-231 cells (A) and 4T1 cells (B). * indicates statistically significant differences (p-value < 0.05) between PCL-ISFIs and 10-CB-ISFI at each incubation time.

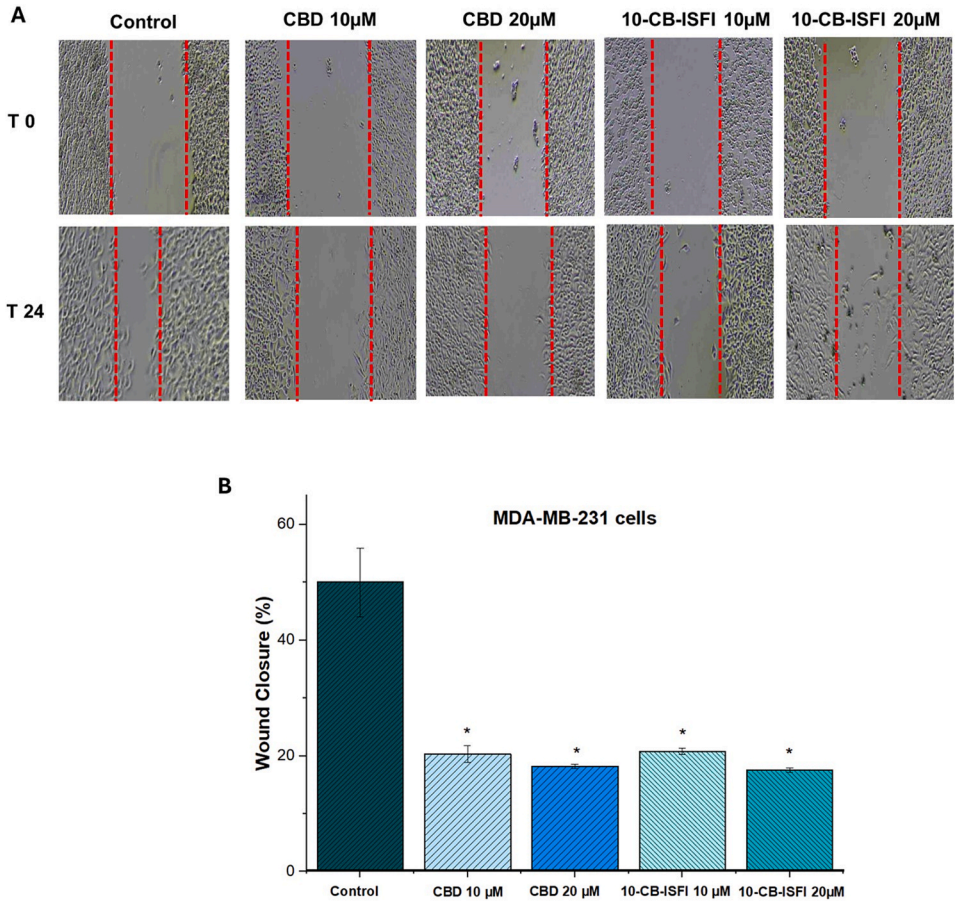

Fig. 5. In vitro scratch wound healing assay in MDA-MB-231 cells. Images at time 0 (T0h) and after 24 h (T24) of treatment (A). Wound closure percentage of each treatment (B). * Indicates statistically significant (p-value < 0.05) differences with the control (cells treated with complete growth medium).

solution. The controlled drug release of CBD can explain this lower activity. The lower effect of the entrapped drug has also been appreciated in viability studies of PLGA microparticles loaded with CBD or paclitaxel in SKOV-3 and A549 cells, respectively (Fraguas-Sánchez et al., 2020a; Kang et al., 2008). In both cases, higher cell death was observed in cells treated with free drug (≈40 and 45 % for paclitaxel and CBD, respectively) than in PLGA-loaded microparticles (≈ 25 % in both cases).

3.3.2. *Migration study: scratch assay*

The migration of cancerous cells from the primary site of the tumor leads to metastasis, which is the main cause of death in cancer patients (Bergers and Fendt, 2021). Its inhibition is an essential step in cancer treatment, and CBD has exhibited an anti-migration activity in some cancer types (O'Reilly et al., 2023). In this study, the effect of CBD-loaded-ISFIs on the migration of TNBC cells has also been evaluated.

Untreated MDA-MB-231 cells (control group) exhibited a wound closure percentage of approximately 50 %. In contrast, cells treated with 10-CB-ISFI showed statistically significant (p-value < 0.01 compared to the control) lower wound closure. It should be noted that CBD-loaded-ISFIs exhibited a similar activity compared with CBD in solution, with wound closure percentages of around 20 % and 17 % at concentrations of 10 μM and 20 μM, respectively (Fig. 5). Significant differences between CBD in solution and 10-CB-ISFI at each concentration were not achieved (p-value > 0.05).

Migration ratios of CBD treatments were also calculated (Table S1). Ratios less than 1 indicate inhibited cell migration, while ratios greater than 1 indicate enhanced migration. Migration ratios of around 0.40 and 0.35 were obtained with both CBD in solution and 10-CB-ISFI at concentrations of 10 μM and 20 μM respectively, corroborating the ability of CBD and CBD-loaded implants to inhibit the migration of MDA-MB-231 cells.

A lower anti-migration activity was detected in 4T1 cells compared to MDA-MB-231 cells. As depicted in Fig. 6A, in the control group of 4T1 cells, the generated wound was almost completely closed, with a closure percentage of around 93 % (Fig. 6B). However, cells treated with CB-ISFIs exhibited a statistically significant (p-value < 0.05) lower wound closure. Like in MDA-MB-231 cells, CBD in solution and 10-CB-ISFI showed a similar and non-statistically significant (p-value > 0.05) effect with wound closure percentages of around 65 % and 57 % at concentrations of 5 μM and 7.5 μM respectively. Migration ratios lower than 1 (around 0.74 and 0.6 at CBD concentrations of 5 μM and 7.5 μM) were appreciated (Table S2).

Other researchers have previously evaluated the effect of CBD on the migration of TNBC cells. In contrast to our data, D'Aoia and collaborators reported that CBD did not have any activity on the migration of MDA-MB-231 cells after 10 h of incubation when administered at concentrations of 5 μM (D'Aloia et al., 2022). Nevertheless, other authors demonstrated its efficacy even at lower concentrations (CBD 2 μM). In

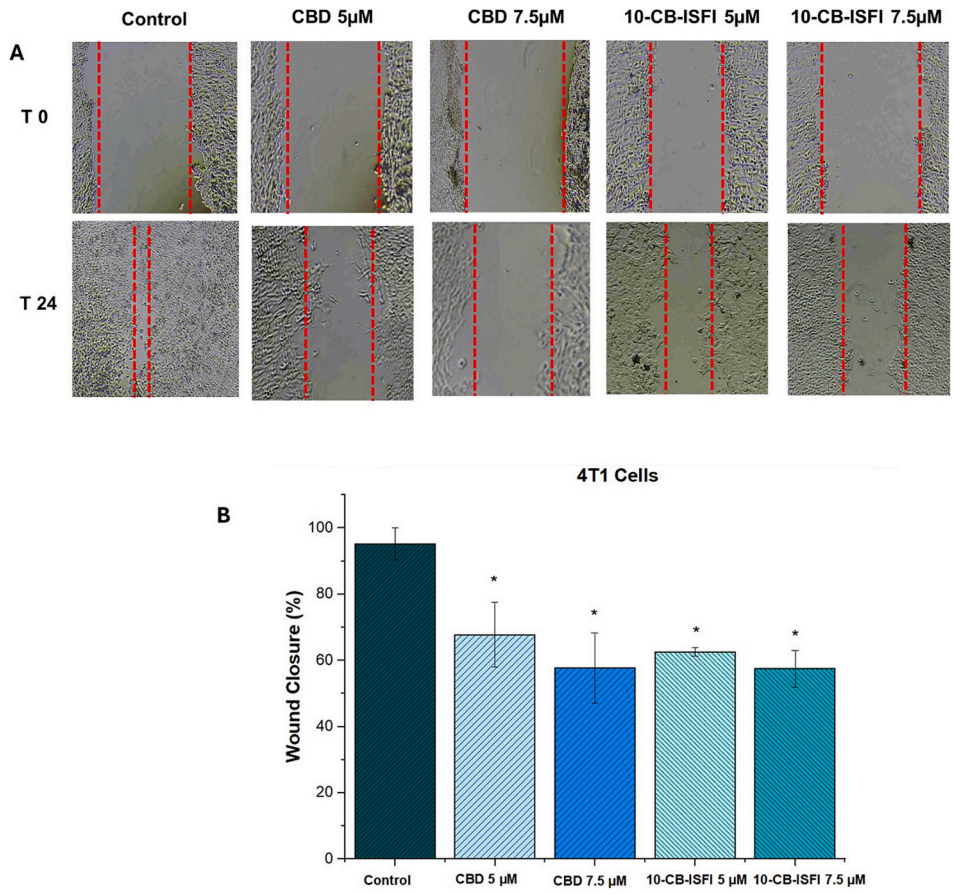

Fig. 6. In vitro scratch wound healing assay in 4T1 cells. Images at time 0 (T0) and after 24 h (T24) of treatment (A). Wound closure percentage of each treatment. * indicates statistically significant (p-value < 0.05) differences with the control (cells treated with complete growth medium).

their study, while non-treated cells exhibited a wound closure of around 60 % after 24 h, cells treated with CBD at 2 μM showed a wound closure of around 40 % (Jo et al., 2021). These results are in accordance with the results of our study, as at 10 μM CBD in solution showed a wound closure percentage of around 20 %. Elbaz and collaborators also evaluated the effect of CBD in the migration of 4T1 cells. In this case, the administration of CBD at 6 μM did not exert any anti-migration activity. However, in this study, the authors used a "transwell model" to evaluate the migration and calculated the migration after 48 h (Elbaz et al., 2015). Using another model could explain the differences found in our study.

3.4. *In ovo studies*

3.4.1. *Angiogenesis studies*

Angiogenesis is a complex and dynamic process crucial for tumor growth and dissemination. Antiangiogenic compounds have become essential in cancer therapy (Liu et al., 2023; Zuazo-Gaztelu and Casanovas, 2018). Several studies have demonstrated the ability of CBD to inhibit angiogenesis (Maia et al., 2023). This study analyzed the antiangiogenic activity of ISFIs using the CAM model.

Implants were successfully formed on the CAM of fertilized chicken eggs. It should be mentioned that CAM assay is a validated model for evaluating the toxicity of drugs and formulations. Notably, 10-CB-ISFIs showed no signs of toxicity, as no damage (e.g., hemorrhage or lysis) was observed, as displayed in Fig. 7A (original image).

Concerning the antiangiogenic activity of 10-CB-ISFI, a statistically significant (p-value < 0.001) lower vascularisation was detected in the eggs treated with the implants compared to the control group (eggs treated with PBS pH 7.4), with vascular density values of around 16 % $\pm$ 1.49 and around 13 % $\pm$ 1.2 in CBD in solution and 10-CB-ISFI treated eggs. Eggs treated with non-loaded implants did not exhibit any effect. Similar and non-statistically significant (p-value > 0.05) vascular density compared with the control (21.5 % $\pm$ 1.3) was obtained. Additionally, it is worth noting that in the eggs treated with unloaded implants (PCL-ISFIs), a similar number of blood vessels was observed compared to the control group (Fig. 7B).

Interestingly, the single administration of 10-CB-ISFIs was more effective than the daily administration of CBD in solution at the same concentration of 100 μM (Fig. 7D). While CBD in solution showed a vascular inhibition percentage of around 65 %, CBD-loaded implants showed an inhibition percentage of around 80 %. However, statistically significant differences between these treatments were not observed (p-value > 0.05). It should be noted that similar data in terms of antiangiogenic effect was also appreciated in the CBD-loaded ISFIs elaborated with PLGA-502 and DMSO (Fischer et al., 2022).

3.4.2. *Antitumor efficacy*

The CAM model offers a straightforward, fast, and cost-effective method for evaluating cancer characteristics, including treatment responses. Tumor cells can be easily grafted onto the CAM, with tumors

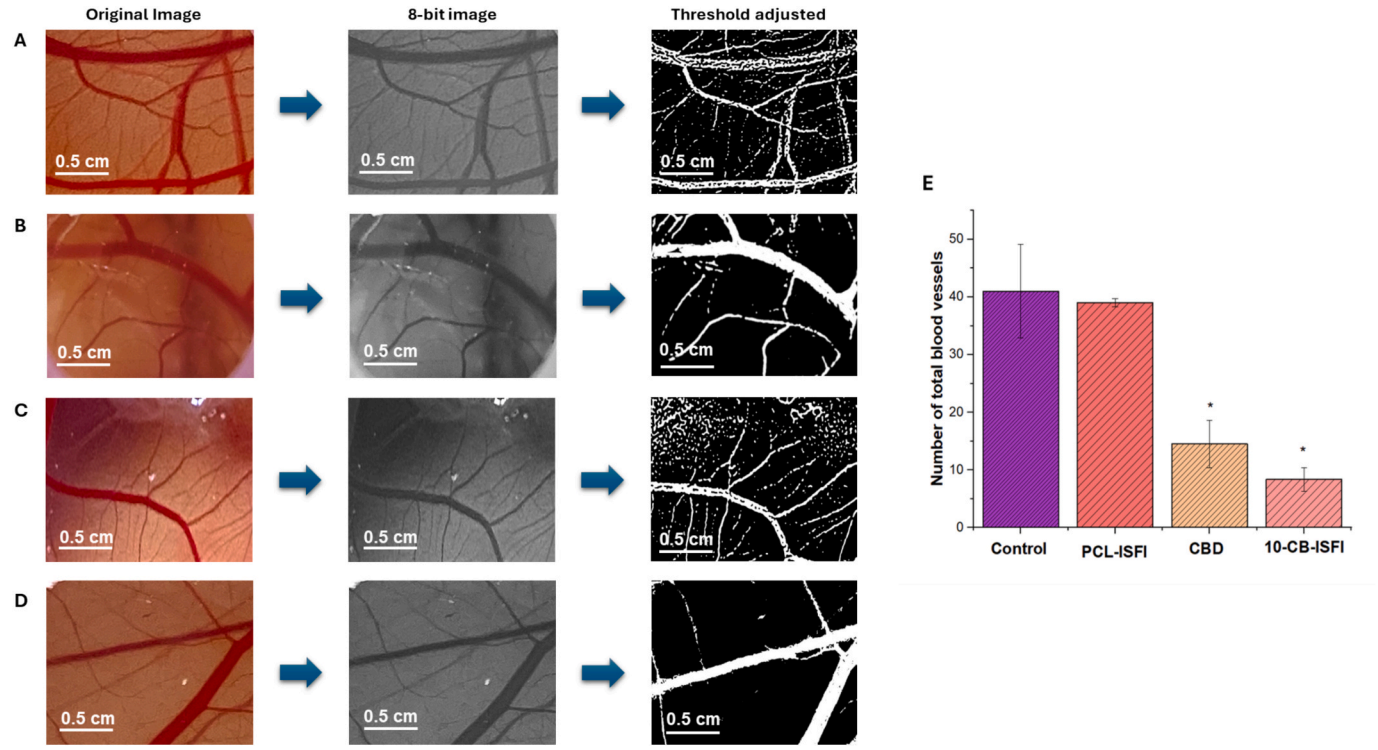

Fig. 7. Angiogenesis study. Original and Image-J-Fiji processed images of the CAM membrane of PBS (control) (A), CBD in solution (B), PCL-ISFI (C) and 10-CB-ISFI (D) treated eggs. Images were captured 24 h after the administration of each treatment. Graph showing the number of total blood vessels (E). * indicates statistically significant (p-value < 0.05) differences between 10-CB-ISFI and the control.

forming rapidly within a few days. Fig. 8A illustrates this model schematically. The anticancer effectiveness of 10-CB-ISFIs was tested on MDA-MB-231-derived tumors developed using this model. MDA-MB-231 cells were selected due to their human origin compared to 4T1 cells, which are murine cells.

48 hours after the treatment, the control group (eggs treated with PBS pH 7.4) showed tumor growth of around 21 %. In contrast, the tumors treated with CBD in solution (7.7 μg of CBD were daily administered) or 10-CB-ISFIs (single administration of a CBD dose of 16 μg) not only stopped their growth but also were reduced by around 60 % (Fig. 8B). Unloaded implants did not exert anticancer activity, with tumor growth percentages slightly higher than the control (≈28 %). Nonetheless, significant differences between the control and PCL-ISFIs were not detected (p-value > 0.05).

CBD is an emerging anti-cancer agent that could potentially be administered in combination with other therapies, such as conventional antineoplastics (Wang and Multhoff, 2021) in many cancer types, including TNBC. The CBD-loaded implant formulations developed in this work proved to be at least as effective as CBD in solution, exerting an antiangiogenic effect and inhibiting the growth of MDA-MB-231-derived tumors.

4. Conclusion

This study presents the development of an injectable CBD formulation capable of forming a depot at the administration site and releasing the drug in an extended manner. Among the tested formulations, the implants prepared with a CBD:PCL ratio of 10:100 exhibited the highest CBD content and the most suitable release profile over two months and demonstrated a significant biological effect against TNBC, inhibiting the migration and proliferation of TNBC cells, reducing tumor growth and decreasing angiogenesis in ovo.

Based on these results, 10-CB-ISFI appears to be a highly promising strategy for the treatment of TNBC. Their single administration at the tumor site could enable a localized and constant release of CBD for at least two months, thereby providing long-lasting anticancer activity. Moreover, since CBD has been shown to enhance the efficacy of several conventional antineoplastic agents used in TNBC treatment, this formulation could potentially be used in combination with current chemotherapeutic regimens. This combination could improve the efficacy of antineoplastic agents, allowing for dose reduction and, consequently, a decrease in associated adverse effects. Given the aggressiveness of TNBC, chemotherapeutic treatments are commonly administered in a neoadjuvant regimen prior to surgery to reduce tumor size and facilitate its removal. In this context, 10-CB-ISFIs could be particularly interesting, as the residual implant would be removed together with the tumor.

Funding sources

Complutense University of Madrid supported this research through researchers Funds (FEI 21/42 and FEI 19/3001) and by the Santander-UCM research group “Formulation and bioavailability of new drug products” (Ref. UCM-910939) (Complutense University of Madrid, Spain). Irene Lozza was awarded a research fellowship, “Perfezionamento all’estero” according to law no. 398 of 1989 – area Cun 05 – Biological science” from Sapienza University of Rome.

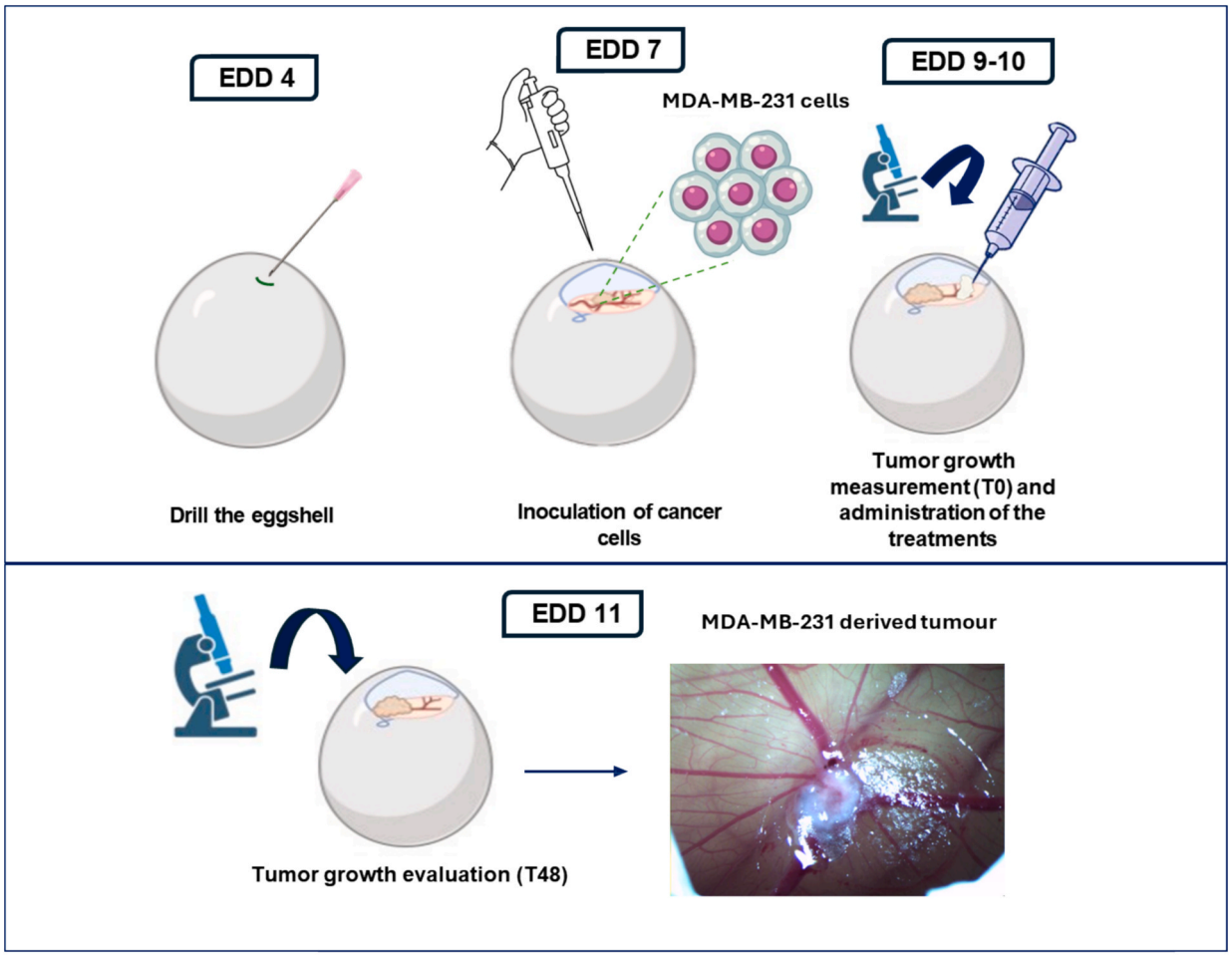

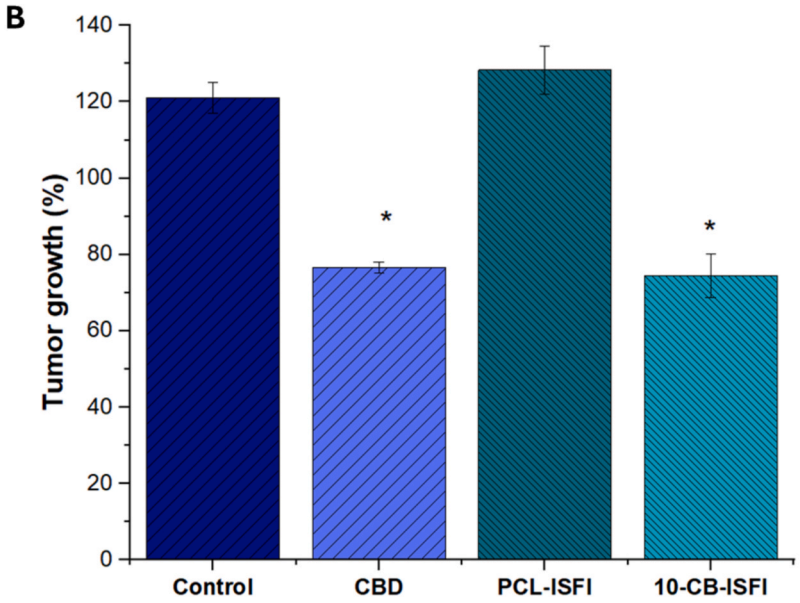

Fig. 8. Schematic representation of tumor formation in the CAM model, including an image of a developed MDA-MB231-derived tumor (A). Tumor growth percentage (%) 48 h after the administration of each treatment. PBS pH 7.4 (control), CBD in solution, PCL-ISFI and 10-CB-ISFI (B). * Symbol shows statistical significance (p-value < 0.05) between 10-CB-ISFI and the control.

CRediT authorship contribution statement

Irene Lozza: Writing – original draft, Investigation, Formal analysis. **Cristina Martín-Sabroso:** Writing – review & editing, Supervision, Investigation, Funding acquisition, Conceptualization. **Carolina Hurtado-Marcos:** Writing – review & editing, Investigation. **Consuelo Montejo-Rubio:** Writing – review & editing, Investigation. **Ana Isabel Fraguas-Sánchez:** Writing – original draft, Supervision, Project

administration, Methodology, Investigation, Formal analysis, Conceptualization, Funding acquisition. **Ana Isabel Torres-Suárez:** Writing – review & editing, Supervision, Methodology, Funding acquisition, Conceptualization.

Declaration of generative AI and AI-assisted technologies in the writing process

During the preparation of this work the author(s) used Grammarly in order to correct and improve the clarity of the manuscript. After using this tool/service, the author(s) reviewed and edited the content as needed and take(s) full responsibility for the content of the publication.

Declaration of competing interest

The authors declare that they have no known competing financial interests or personal relationships that could have appeared to influence the work reported in this paper.

Appendix A. Supplementary data

Supplementary data to this article can be found online at https://doi.org/10.1016/j.ijpharm.2025.125710.

Data availability

The authors are unable or have chosen not to specify which data has been used.

References

Alonso-González, M., Fernández-Carballido, A., Quispe-Chauca, P., Lozza, I., Martín-Sabroso, C., Isabel Fraguas-Sánchez, A., 2022. DoE-based development of celecoxib loaded PLGA nanoparticles: in ovo assessment of its antiangiogenic effect. Eur. J. Pharm. Biopharm. 180, 149–160.

Barzaman, K., Karami, J., Zarei, Z., Hosseinzadeh, A., Kazemi, M.H., Moradi-Kalbolandi, S., Safari, E., Farahmand, L., 2020. Breast cancer: biology, biomarkers, and treatments. Int. Immunopharmacol. 84, 106535.

Bathula, P.P., Maciver, M.B., 2024. Cannabinoids in treating chemotherapy-induced nausea and vomiting, cancer-associated pain, and tumor growth. Int. J. Mol. Sci. 25, 74.

Bergers, G., Fendt, S.-M., 2021. The metabolism of cancer cells during metastasis. Nat. Rev. Cancer 21, 162–180.

Bhadran, A., Shah, T., Babanyinah, G.K., Polara, H., Taslimy, S., Biewer, M.C., Stefan, M. C., 2023. Recent advances in polycaprolactones for anticancer drug delivery. Pharmaceutics 15.

Bimonte, S., Nocerino, D., Schiavo, D., Crisci, M., Cascella, M., Cuomo, A., 2024. Cannabinoids for cancer-related pain management: an update on therapeutic applications and future perspectives. Anticancer Res. 44, 895–900.

Bimonte, S., Palma, G., Cascella, M., Cuomo, A., 2023. Phytocannabinoids in triple negative breast cancer treatment: current knowledge and future insights. Anticancer Res. 43, 993–1000.

Bray, F., Laversanne, M., Sung, H., Ferlay, J., Siegel, R.L., Soerjomataram, I., Jemal, A., 2024. Global cancer statistics 2022: GLOBOCAN estimates of incidence and mortality worldwide for 36 cancers in 185 countries. CA Cancer J. Clin. 74, 229–263.

Buchtova, T., Lukac, D., Skrott, Z., Chroma, K., Bartek, J., Mistrik, M., 2023. Drug-drug interactions of cannabidiol with standard-of-care chemotherapeutics. Int. J. Mol. Sci. 24.

Clusan, L., Le Goff, P., Flouriot, G., Pakdel, F., 2021. A closer look at estrogen receptor mutations in breast cancer and their implications for estrogen and antiestrogen responses. Int. J. Mol. Sci. 22.

Coelho, M.P., Duarte, P., Calado, M., Almeida, A.J., Reis, C.P., Gaspar, M.M., 2023. The current role of cannabis and cannabinoids in health: a comprehensive review of their therapeutic potential. Life Sci. 329, 121838.

D'Aloia, A., Ceriani, M., Tisi, R., Stucchi, S., Sacco, E., Costa, B., 2022. Cannabidiol antiproliferative effect in triple-negative breast cancer MDA-MB-231 cells is modulated by its physical state and by IGF-1. Int. J. Mol. Sci. 23.

Dubar, M., Lizambard, M., Delcourt-Debruyne, E., Batool, F., Huck, O., Siepmann, F., Agossa, K., 2021. In-situforming drug-delivery systems for periodontal treatment: current knowledge and perspectives. Biomed. Mater. 16.

Duchesne, C., Frescaline, N., Lataillade, J.-J., Rousseau, A., 2018. Comparative study between direct and indirect treatment with cold atmospheric plasma on in vitro and in vivo models of wound healing. 8, 379–401.

Elbaz, M., Nasser, M.W., Ravi, J., Wani, N.A., Ahirwar, D.K., Zhao, H., Oghumu, S., Satoskar, A.R., Shilo, K., Carson 3rd, W.E., Ganju, R.K., 2015. Modulation of the tumor microenvironment and inhibition of EGF/EGFR pathway: novel anti-tumor mechanisms of Cannabidiol in breast cancer. Mol. Oncol. 9, 906–919.

Fischer, D., Fluegen, G., Garcia, P., Ghaffari-Tabrizi-Wizsy, N., Gribaldo, L., Huang, R.Y., Rasche, V., Ribatti, D., Rousset, X., Pinto, M.T., Viallet, J., Wang, Y., Schneider-Stock, R., 2022. The CAM model-Q&A with experts. Cancers (Basel) 15.

Fraguas-Sánchez, A.I., Fernández-Carballido, A., Delie, F., Cohen, M., Martin-Sabroso, C., Mezzanzanica, D., Figini, M., Satta, A., Torres-Suárez, A.I., 2020a. Enhancing ovarian cancer conventional chemotherapy through the combination with cannabidiol loaded microparticles. Eur. J. Pharm. Biopharm. 154, 246–258.

Fraguas-Sánchez, A.I., Fernández-Carballido, A., Martin-Sabroso, C., Torres-Suárez, A.I., 2020b. Stability characteristics of cannabidiol for the design of pharmacological, biochemical and pharmaceutical studies. J. Chromatogr. B Anal. Technol. Biomed. Life Sci. 1150, 122188.

Fraguas-Sánchez, A.I., Fernández-Carballido, A., Torres-Suárez, A.I., 2023. Chapter 29 – Cannabidiol (CBD) use in breast cancer chemotherapy. In: Preedy, V.R., Patel, V.B., Martin, C.R. (Eds.), Medicinal Usage of Cannabis and Cannabinoids. Academic Press, pp. 373–383.

Fraguas-Sánchez, A.I., Hernán, D., Montejo, C., Poklis, J.L., Lichtman, A.H., Torres-Suárez, A.I., 2024. Polycaprolactone microparticles for the subcutaneous administration of cannabidiol: in vitro and in vivo release. Drug Deliv. Transl. Res. 14, 959–969.

Fraguas-Sánchez, A.I., Torres-Suárez, A.I., Cohen, M., Delie, F., Bastida-Ruiz, D., Yart, L., Martin-Sabroso, C., Fernández-Carballido, A., 2020c. PLGA nanoparticles for the intraperitoneal administration of CBD in the treatment of ovarian cancer: in vitro and in ovo assessment. Pharmaceutics 12.

Fraguas Sánchez, A., Torres-Suarez, A., 2023. Therapeutic uses of Cannabis sativa L. Current State and Future Perspectives 407–445.

García-Escolano, M., Montoyo-Pujol, Y.G., Ortiz-Martínez, F., Ponce, J.J., Delgado-Garcia, S., Martin, T.A., Ballester, H., Aranda, F.I., Castellon-Molla, E., Sempere Ortells, J.M., Peiró, G., ID1 and ID4 are biomarkers of tumor aggressiveness and poor outcome in immunophenotypes of breast cancer.

Gentile, P., Chiono, V., Carmagnola, I., Hatton, P.V., 2014. An overview of poly(lactic-co-glycolic) acid (PLGA)-based biomaterials for bone tissue engineering. Int. J. Mol. Sci. 15, 3640–3659.

Gomaa, E., Eissa, N.G., Ibrahim, T.M., El-Bassossy, H.M., El-Nahas, H.M., Ayoub, M.M., 2023. Development of depot PLGA-based in-situ implant of Linagliptin: sustained release and glycemic control. Saudi Pharm. J. 31, 499–509.

Hao, E., Mukhopadhyay, P., Cao, Z., Erdélyi, K., Holovac, E., Liaudet, L., Lee, W.S., Haskó, G., Mechoulam, R., Pacher, P., 2015. Cannabidiol protects against doxorubicin-induced cardiomyopathy by modulating mitochondrial function and biogenesis. Mol. Med. 21, 38–45.

Heider, C.G., Itenberg, S.A., Rao, J., Ma, H., Wu, X., 2022. Mechanisms of cannabidiol (CBD) in cancer treatment: a review. Biology (Basel) 11.

Ibrahim, T.M., El-Megrab, N.A., El-Nahas, H.M., 2021. An overview of PLGA in-situ forming implants based on solvent exchange technique: effect of formulation components and characterization. Pharm. Dev. Technol. 26, 709–728.

Jensen, S.S., Jensen, H., Møller, E.H., Cornett, C., Siepmann, F., Siepmann, J., Østergaard, J., 2016. In vitro release studies of insulin from lipid implants in solution and in a hydrogel matrix mimicking the subcutis. Eur. J. Pharm. Sci. 81, 103–112.

Jo, M.J., Kim, B.G., Kim, W.Y., Lee, D.H., Yun, H.K., Jeong, S., Park, S.H., Kim, B.R., Kim, J.L., Kim, D.Y., Lee, S.I., Oh, S.C., 2021. Cannabidiol suppresses angiogenesis and stemness of breast cancer cells by downregulation of hypoxia-inducible factors-1α. Cancers (Basel) 13.

Kang, Y., Wu, J., Yin, G., Huang, Z., Liao, X., Yao, Y., Ouyang, P., Wang, H., Yang, Q., 2008. Characterization and biological evaluation of paclitaxel-loaded poly(l-lactic acid) microparticles prepared by supercritical CO2. Langmuir 24, 7432–7441.

Kanwar, N., Sinha, V.R., 2019. In situ forming depot as sustained-release drug delivery systems. Crit. Rev. Ther. Drug Carrier Syst. 36, 93–136.

Kumar Kalvala, A., Bagde, A., Arthur, P., Kumar Surapaneni, S., Ramesh, N., Nathani, A., Singh, M., 2022. Role of Cannabidiol and Tetrahydrocannabivarin on Paclitaxel-induced neuropathic pain in rodents. Int. Immunopharmacol. 107, 108693.

Lim, Y.W., Tan, W.S., Ho, K.L., Mariatulqabtiah, A.R., Abu Kasim, N.H., Abd. Rahman, N., Wong, T.W., Chee, C.F., 2022. Challenges and complications of poly (lactic-co-glycolic acid)-based long-acting drug product development. Pharmaceutics 14, 614.

Liu, Z.L., Chen, H.H., Zheng, L.L., Sun, L.P., Shi, L., 2023. Angiogenic signaling pathways and anti-angiogenic therapy for cancer. Signal Transduct. Target. Ther. 8, 198.

Lozza, I., Martín-Sabroso, C., Torres-Suárez, A.I., Fraguas-Sánchez, A.I., 2024. In situ forming PLA and PLGA implants for the parenteral administration of Cannabidiol. Int. J. Pharm. 661, 124468.

Maia, J., Fonseca, B.M., Teixeira, N., Correia-da-Silva, G., 2023. Unveiling the angiogenic effects of cannabinoids: enhancers or inhibitors? Biochem. Pharmacol. 215, 115686.

Markowicz-Piasecka, M., Kubisiak, M., Asendrych-Wicik, K., Kołodziejczyk, M., Grzelińska, J., Fabijańska, M., Pietrzak, T., 2024. Long-acting injectable antipsychotics—a review on formulation and in vitro dissolution. Pharmaceutics 16, 28.

Miles, C.E., Bernstein, A.D., Osborn Popp, T.M., Murthy, N.S., Nieuwkoop, A.J., Gormley, A.J., 2021. Control of drug release from microparticles by tuning their crystalline textures: a structure–activity study. ACS Appl. Polym. Mater. 3, 6548–6561.

Nahler, G., 2022. Cannabidiol and other phytocannabinoids as cancer therapeutics. Pharmaceut. Med. 36, 99–129.

O'Reilly, E., Khalifa, K., Cosgrave, J., Azam, H., Prencipe, M., Simpson, J.C., Gallagher, W.M., Perry, A.S., 2023. Cannabidiol inhibits the proliferation and invasiveness of prostate cancer cells. J. Nat. Prod. 86, 2151–2161.

Obidiro, O., Battogtokh, G., Akala, E.O., 2023. Triple negative breast cancer treatment options and limitations: future outlook. Pharmaceutics 15.
Pandya, A.K., Vora, L.K., Umeyor, C., Surve, D., Patel, A., Biswas, S., Patel, K., Patravale, V.B., 2023. Polymeric in situ forming depots for long-acting drug delivery systems. Adv. Drug Deliv. Rev. 200, 115003.
Patel, N., Kommineni, N., Surapaneni, S.K., Kalvala, A., Yaun, X., Gebeyehu, A., Arthur, P., Duke, L.C., York, S.B., Bagde, A., Meckes Jr., D.G., Singh, M., 2021. Cannabidiol loaded extracellular vesicles sensitize triple-negative breast cancer to doxorubicin in both in-vitro and in vivo models. Int. J. Pharm. 607, 120943.
Pawar, R., Pathan, A., Nagaraj, S., Kapare, H., Giram, P., Wavhale, R., 2023. Polycaprolactone and its derivatives for drug delivery. Polym. Adv. Technol. 34, 3296–3316.
Sabaner, M.C., Duman, R., Vurmaz, A., Ertekin, T., 2021. Effects of topical prostaglandin drops on angiogenesis in an in ovo chick chorioallantoic membrane model. Cutan. Ocul. Toxicol. 40, 54–60.
Skórzewska, M., Gęca, K., 2024. The role of cannabinoids in advancing cancer treatment: insights from evidence-based medicine. Curr. Oncol. Rep.
Suh, M.S., Kastellorizios, M., Tipnis, N., Zou, Y., Wang, Y., Choi, S., Burgess, D.J., 2021. Effect of implant formation on drug release kinetics of in situ forming implants. Int. J. Pharm. 592, 120105.
Sukumar, J., Gast, K., Quiroga, D., Lustberg, M., Williams, N., 2021. Triple-negative breast cancer: promising prognostic biomarkers currently in development. Expert Rev. Anticancer Ther. 21, 135–148.
Surapaneni, S.K., Patel, N., Sun, L., Kommineni, N., Kalvala, A.K., Gebeyehu, A., Arthur, P., Duke, L.C., Nimma, R., Meckes Jr, G.D., 2022. Anticancer and chemosensitization effects of cannabidiol in 2D and 3D cultures of TNBC: involvement of GADD45α, integrin-α5,-β5,-β1, and autophagy. Drug Deliv. Transl. Res. 12, 2762–2777.
Thakur, R.R.S., McMillan, H.L., Jones, D.S., 2014. Solvent induced phase inversion-based in situ forming controlled release drug delivery implants. J. Control. Release 176, 8–23.
Ulhaka, K., Kanokwiroon, K., Khongkow, M., Bissanum, R., Khunpitak, T., Khongkow, P., 2021. The anticancer effects of FDI-6, a FOXM1 inhibitor, on triple negative breast cancer. Int. J. Mol. Sci. 22.
Wang, F., Multhoff, G., 2021. Repurposing Cannabidiol as a potential drug candidate for anti-tumor therapies. Biomolecules 11.
Wang, X., Burgess, D.J., 2021. Drug release from in situ forming implants and advances in release testing. Adv. Drug Deliv. Rev. 178, 113912.
Xiong, N., Wu, H., Yu, Z., 2024. Advancements and challenges in triple-negative breast cancer: a comprehensive review of therapeutic and diagnostic strategies. Front. Oncol. 14.
Yan, C., Li, Y., Liu, H., Chen, D., Wu, J., 2023. Antitumor mechanism of cannabidiol hidden behind cancer hallmarks. Biochim. Biophys. Acta 1878, 188905.
Yin, L., Duan, J.-J., Bian, X.-W., Yu, S.-C., 2020. Triple-negative breast cancer molecular subtyping and treatment progress. Breast Cancer Res. 22, 61.
Young, I.C., Massud, I., Cottrell, M.L., Shrivastava, R., Maturavongsadit, P., Prasher, A., Wong-Sam, A., Dinh, C., Edwards, T., Mrotz, V., Mitchell, J., Seixas, J.N., Pallerla, A., Thorson, A., Schauer, A., Sykes, C., De la Cruz, G., Montgomery, S.A., Kashuba, A.D. M., Heneine, W., Dobard, C.W., Kovarova, M., Garcia, J.V., García-Lerma, J.G., Benhabbour, S.R., 2023. Ultra-long-acting in-situ forming implants with cabotegravir protect female macaques against rectal SHIV infection. Nat. Commun. 14, 708.
Zhang, X., Yang, L., Zhang, C., Liu, D., Meng, S., Zhang, W., Meng, S., 2019. Effect of polymer permeability and solvent removal rate on in situ forming implants: drug burst release and microstructure. Pharmaceutics.
Zuazo-Gaztelu, I., Casanovas, O., 2018. Unraveling the role of angiogenesis in cancer ecosystems. Front. Oncol. 8, 248.